

Extended x-ray absorption fine-structure study of hydrogenated amorphous silicon-germanium alloys

L. Incoccia* and S. Mobilio

Progetto per l'Utilizzazione della Luce di Sincrotrone, Istituto Nazionale di Fisica Nucleare, Laboratori Nazionali di Frascati, 00044 Frascati (Roma), Italy

M. G. Proietti, P. Fiorini, C. Giovannella, and F. Evangelisti
Dipartimento di Fisica, Università La Sapienza, 00185 Roma, Italy

(Received 12 June 1984)

The local structure of hydrogenated amorphous Ge-Si alloys has been studied by measuring the x-ray absorption at the Ge *K* edge. Ge-Ge and Ge-Si distances were found to be independent of concentration and equal to 2.45 and 2.38 Å, respectively. A study of the composition of the first coordination shell around Ge is consistent with a random mixing of the two species in the alloys. The total disorder factors have been determined for both Ge-Ge and Ge-Si, and they turned out to be constant and equal to each other over the whole concentration range studied.

I. INTRODUCTION

The possibility of "tailoring" optical and electronic properties makes the study of the semiconducting binary alloys of great interest. This is even more true for hydrogenated amorphous tetrahedral semiconductors due to the flexibility of the deposition processes by, e.g., glow discharge, and to the complete miscibility of the elements. In particular, the hydrogenated amorphous silicon-germanium alloys ($a\text{-Ge}_x\text{Si}_{1-x}\text{:H}$) have been recently extensively studied¹ and applied in efficient photovoltaic devices.²

Generally speaking, however, the alloys tend to have more defects and localized states in the gap than the elementary films do, an occurrence pointing to additional disorder present in the amorphous matrix. In order to shed light on these problems, a close examination of the local structure is of paramount importance. To this end, extended x-ray absorption fine structure (EXAFS) is the best suited technique due to its unique capability of investigating the surroundings of single atomic species.³ In the present work, we have measured EXAFS spectra above the Ge *K* edge in a series of hydrogenated amorphous silicon-germanium alloys as a function of their relative composition. Two main points are clarified by the analysis. First, Ge-Ge and Ge-Si distances are, respectively, 2.45 and 2.38 Å and do not vary with composition, a result implying an additional distortion of the amorphous network in the alloys as compared to the elementary films. Second, we found a random composition of the first-neighbor shell, implying a compositional disorder superimposed on the topological one. Both results qualitatively account for the larger number of localized electronic states present in these alloys.

II. EXPERIMENTAL

The samples were grown in a rf capacitively coupled glow-discharge apparatus by a mixture of SiH_4 and GeH_4 .

The gas composition $r = [\text{GeH}_4]/([\text{SiH}_4] + [\text{GeH}_4])$ was varied in the range 0–0.93. The deposition temperature was 250°C, but few samples were also deposited at 190°C. The chemical composition x was determined by plasma emission spectroscopy at CISE Laboratories, Segrate, Italy. The results are shown in Fig. 1, where a higher deposition rate of Ge is apparent. The continuous line is the result⁴ of a best fit assuming an independent deposition rate for the two species. The best agreement with the experimental points is found for a value equal to 3 for the ratio between the sticking coefficient of Ge and Si.

The x-ray absorption spectra at the Ge *K* edge were taken at the Frascati Synchrotron Radiation facility. The radiation emitted by the ADONE storage ring ($E = 1.5$ GeV, average current $I_A \cong 50$ mA) was monochromatized by a Si(111) channel-cut crystal. The average photon (ph) flux was $\sim 10^9$ ph/s and the resolution ~ 2 eV.⁵ The samples were held in vacuum and the spectra were taken at

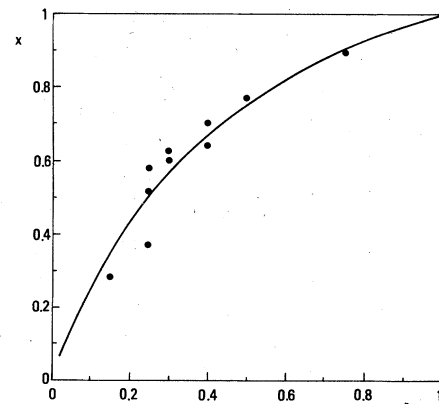


FIG. 1. Relative concentration x of germanium as determined by chemical analysis of the samples vs the gas composition in the glow-discharge apparatus $r = [\text{GeH}_4]/([\text{GeH}_4] + [\text{SiH}_4])$.

room temperature. Particular care was devoted to avoid any experimental artifact that could affect the EXAFS amplitudes, such as inhomogeneities in the samples or misalignment of the whole setup.^{6,7}

III. EXAFS RESULTS AND ANALYSIS

In Fig. 2 we show the EXAFS spectra of the samples studied. It is apparent that the line shapes of the two extreme cases [spectra (a) and (h) corresponding to $x=0.07$ and $x=1$, respectively] are quite different: spectrum (a) having a monotonically decreasing envelope function, spectrum (h) a nearly Gaussian envelope function with a maximum at $\sim 7 \text{ \AA}^{-1}$. This dissimilar k dependence results from the different backscattering function⁸ of the atoms which form the first coordination shell in the two cases: Ge in spectrum (h) and predominantly Si in spectrum (a).

With decreasing Ge concentration the remaining spectra of Fig. 2 exhibit a progressive evolution toward a higher backscattering amplitude at low k and a decrease of the maximum at $\sim 7 \text{ \AA}^{-1}$. This behavior confirms a smooth variation of the first-shell composition from pure Ge to pure Si.

Upon Fourier transforming the spectra, one gets the radial distribution function centered at the absorbing atoms.⁹ They are shown in Fig. 3 for three different concentrations. Only the first-shell contribution due to the

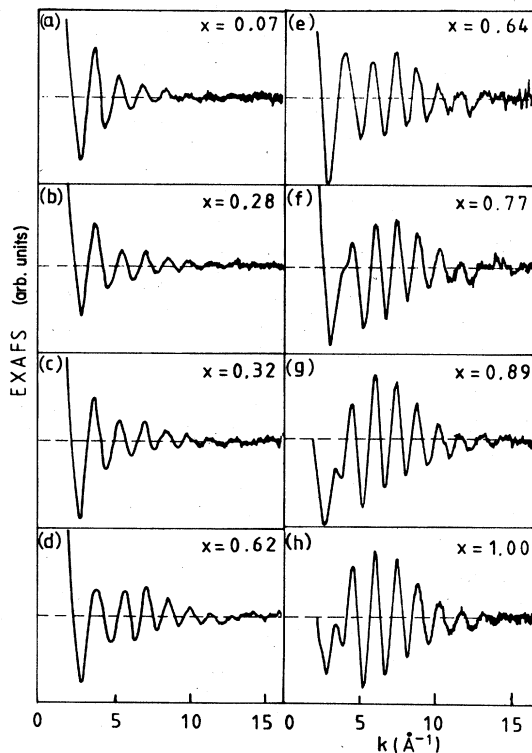


FIG. 2. Experimental $\chi(k)$ at different Ge concentrations: the interference function was obtained by subtracting a cubic fit curve to the experimental absorption coefficient $\mu(k)$. The zero of the kinetic energy E_0 was assumed at the inflection point of the Ge K edge.

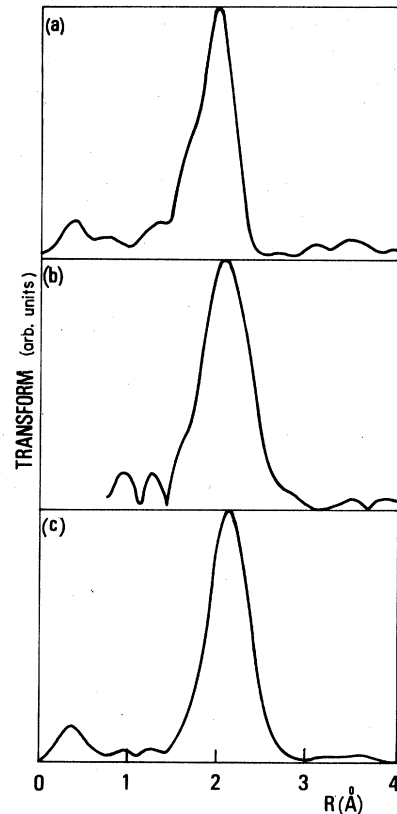


FIG. 3. Fourier transform of EXAFS spectra corresponding to (a) $x=0.07$, (b) $x=0.64$, (c) $x=1$. The transformation range used was the same for the whole set of samples and equal to $2.5 \div 15 \text{ \AA}^{-1}$. A k -weighting factor and a Gaussian window were used.

nearest neighbors is present, without any significant structure at higher- R values, pointing to the lack of long-range order in these alloys. In the pure hydrogenated amorphous germanium (a -Ge:H) samples the peak position, corrected by the phase shift, corresponds to the Ge-Ge bond length of $R=2.45 \text{ \AA}$. With decreasing Ge content the peak position shifts towards lower- R values, with a "mean" linear dependence on x as shown in Fig. 4.

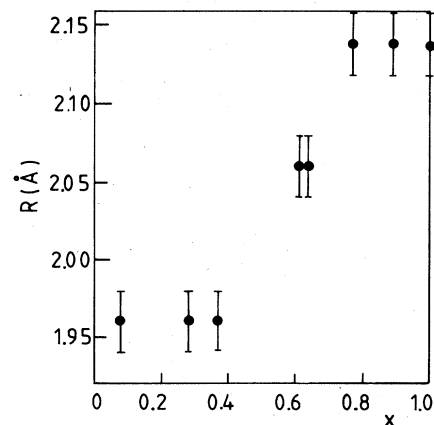


FIG. 4. Plot of the FT maxima vs x , not corrected for the two-phase shift.

However, we found in a preliminary analysis of the spectra performed in k space that these Fourier-transformed peaks could be composed by two contributions: Ge-Ge and Ge-Si pairs whose bond lengths and relative weight should be determined. It is to be noted that the two pairs contribute to the Fourier transform (FT) peaks with different phase shifts and with different weights due not only to the chemical composition of the first-coordination shell but also to the backscattering amplitudes. These two contributions are not resolved in R space owing to the broadening introduced by the finite transformation range and to the Gaussian window used in the transform.¹⁰ In order to unfold them we performed a complete k -space analysis by transforming back the first Fourier peak. By this backtransforming procedure we regained the EXAFS spectra filtered from the noise:¹¹

$$\chi(K) = \sum_{n:\text{Si,Ge}} \frac{N_n}{kR_n^2} S_0^2 |f_n(k, \pi)| e^{-2k^2\sigma_n^2} \times \sin[2kR_n + \phi_n(k)], \quad (1)$$

where the sum extends over the two species of backscattering atoms, N_n is the number of Ge or Si atoms in the first coordination shell, R_n is the bond length of the pair Ge-Ge or Ge-Si, σ_n^2 is the rms fluctuation of R_n including the thermal and static contribution, $|f(k, \pi)|$ is the backscattering function of Ge or Si, $\phi_n(k)$ is the phase-shift function including both the central atom phase shift and the backscattering one, and S_0^2 accounts for the many-body relaxation effects.¹² In order to extract structural information (i.e., N_n, R_n , and σ_n^2 for both pairs) from Eq. (1), it is necessary to know the backscattering amplitudes and phases of the two-atom pairs involved. This is generally done by using model compounds provided they are as close as possible to the unknown systems in terms of chemical bond, geometry, and bond distances.^{13,14} In our case, the EXAFS spectra of the samples with the two extreme compositions $x=1$ and 0.07 are the obvious representatives of Ge-Ge and Ge-Si pairs, respectively. These two samples match all the conditions required to be good models for investigating the alloys with intermediate compositions. Therefore, a complete study of these two materials was in order. In what follows we report the results of this characterization and then the analysis on the different alloys.

A. a -GeH case

Many EXAFS investigations have been performed on evaporated and sputtered a -Ge (Refs. 15–21) but no study has been done on a -Ge:H grown by glow discharge. The main results we obtained are the following.

(a) The bond length Ge–Ge was determined in two ways: from the Fourier transform, which, as mentioned previously, peaks at the same position as in the crystalline Ge (c -Ge), and from a comparison of the total phase $\pi(k)=2kR + \phi(k)$ of pure a -Ge:H with that of c -Ge. Both methods give $R=2.45$ Å as in c -Ge and a -Ge. Notice that in the present work the value for E_0 has been assumed to be equal to the energy position of the main in-

flexion point of the Ge K edge.

(b) The envelope function of the experimental spectra

$$A(k) = (S_0^2 N / R^2) \exp(-2\sigma^2 k^2) |f(k, \pi)|$$

was compared with several simulated envelope functions, obtained using the theoretical $|f(k, \pi)|$ calculated by Teo and Lee⁸ and different trial values for S_0^2 and σ^2 . The best agreement was obtained with $S_0^2=0.67$ and $\sigma^2=0.5 \times 10^{-2}$ Å² (Fig. 5). The value for S_0^2 is in close agreement with previous results.¹²

(c) The coordination number $N_{a\text{-Ge:H}}$ and the disorder factor σ^2 have been deduced from the plot of the function $\ln[A_{a\text{-Ge:H}}(k)/A_{c\text{-Ge}}(k)]$ versus k^2 . As known,²² this function has a linear behavior whose value at $k^2=0$ is equal to the ratio $\ln[N_{a\text{-Ge:H}}(k)/N_{c\text{-Ge}}(k)]$ and whose slope is $\Delta\sigma^2 = -2(\sigma_{a\text{-Ge:H}}^2 - \sigma_{c\text{-Ge}}^2)$. In Fig. 6 we show this plot obtained from our experimental data. The oscillations of the experimental curve around the best-fitted linear behavior are very small over a large- k range and point to the good quality of the data. The accuracy of this determination of N and σ^2 was established²³ to be 5% and 10%, respectively. We find $N_{a\text{-Ge:H}}=4.0 \pm 0.2$ and $\Delta\sigma^2=(0.16 \pm 0.015) \times 10^{-2}$ Å². Since σ^2 for c -Ge is $(0.33 \pm 0.01) \times 10^{-2}$ Å²,²⁴ the disorder factor results $(0.49 \pm 0.025) \times 10^{-2}$ Å⁻².

B. a -Ge _{x} Si _{$1-x$} :H case

In this case the EXAFS spectra are practically determined by the Si backscattering function since the contribution of Ge atoms to the Ge first-nearest-neighbor shell, averaged over the entire sample, should be no more than 7%. This Ge contribution is certainly close to the sensitivity of the technique. Nevertheless, in order to obtain unambiguously the EXAFS of the Ge-Si pair, we have subtracted from the experimental data the a -Ge:H spectrum multiplied by the statistical weight $\frac{6}{99}=0.06$. Then, after Fourier filtering, we compared these experimental backscattering amplitude and phase functions with the theoretical ones calculated for Si.⁸ In the theoretical spectrum a coordination number $N=4$ has been assumed, as suggested by the pure a -Ge:H sample for which the coordination is the same as in the crystal. In Fig. 7 we show the difference between the experimental and theoretical total phases as a function of k . The linear behavior ob-

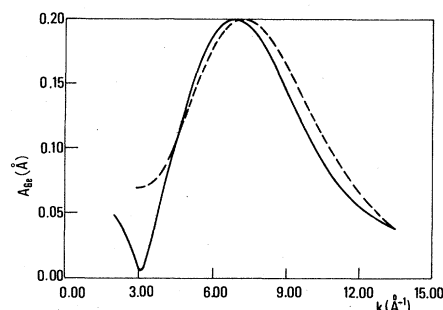


FIG. 5. Backscattering amplitude of Ge. Solid curve: experimental, obtained by backtransforming the FT peak of the a -Ge:H sample. Dashed line: theoretical, obtained by using Teo and Lee's parameters.

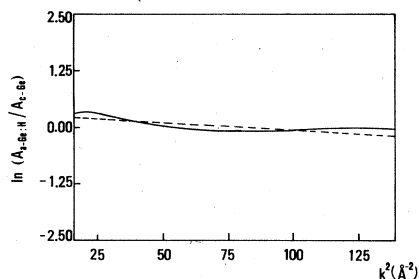


FIG. 6. $\ln[A_{a\text{-Ge:H}}(k)/A_{c\text{-Ge}}(k)]$ vs k at room temperature. The straight line was obtained by a linear fit in the range $k^2=25 \div 125 \text{ \AA}^2$.

tained over the entire experimental k range demonstrates the excellent agreement between theoretical and experimental phases and that the Ge-Si distance is $2.38 \pm 0.01 \text{ \AA}$ in this compound.

As for the amplitudes, the same procedure outlined in the $a\text{-Ge:H}$ case was followed. Figure 8 shows the good match between the experiment and theory, provided the latter is corrected by an overlap factor $S_0^2=0.6$ and the disorder factor $\exp(-2k\sigma^2)$ with $\sigma^2=0.5 \times 10^{-2} \text{ \AA}^2$. It is to be noted that the σ^2 value obtained is equal to the total σ^2 in $a\text{-Ge:H}$. Since the overlap factor depends only on multiple excitations of the central atom,¹² the S_0^2 value found seemed to be low as compared with the value 0.67 found for the $a\text{-Ge:H}$ sample. This discrepancy is probably due to the approximations needed for the theoretical amplitude calculations, which are less valid when the atomic number of the element decreases.

C. Results on the alloys

From the previous study we obtained the phase and amplitude functions for the Ge-Ge and Ge-Si pairs that can be used for the analysis of the EXAFS spectra of the remaining alloys at intermediate concentrations. With these phases and amplitudes a fitting function was built in k space to be compared to Fourier filtered $k\chi(k)$. The only assumption we did is that the average coordination number around the Ge atoms does not vary as a function of the concentration. This hypothesis is reasonable since in both the two extreme cases considered ($x=1$ and 0.07) the coordination number was equal to 4. Therefore we performed a two-shells fit by keeping fixed the total coor-

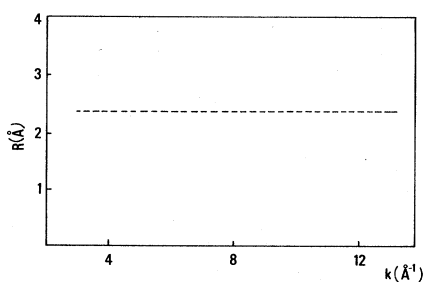


FIG. 7. Ge-Si nearest-neighbor distance obtained from the difference between the theoretical and experimental phases in the $\text{Ge}_{0.07}\text{Si}_{0.93}\text{:H}$ sample.

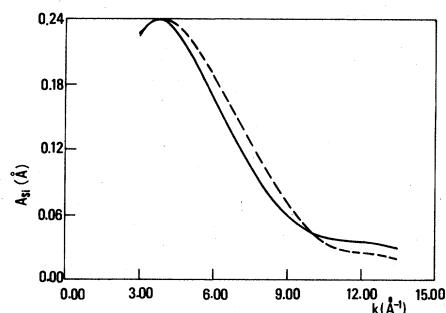


FIG. 8. Backscattering amplitude of Si. Solid curve: experimental, obtained by backtransforming the FT peak of the $a\text{-Ge}_{0.07}\text{Si}_{0.93}$ alloy. Dashed line: theoretical, obtained by using Teo and Lee's parameters.

dination number around the Ge atoms, but varying the relative concentration of the two components, their σ^2 factors and R values. In Fig. 9 we show the excellent quality of the fits obtained, and in Table I we report the numerical results. We want to stress here the following:

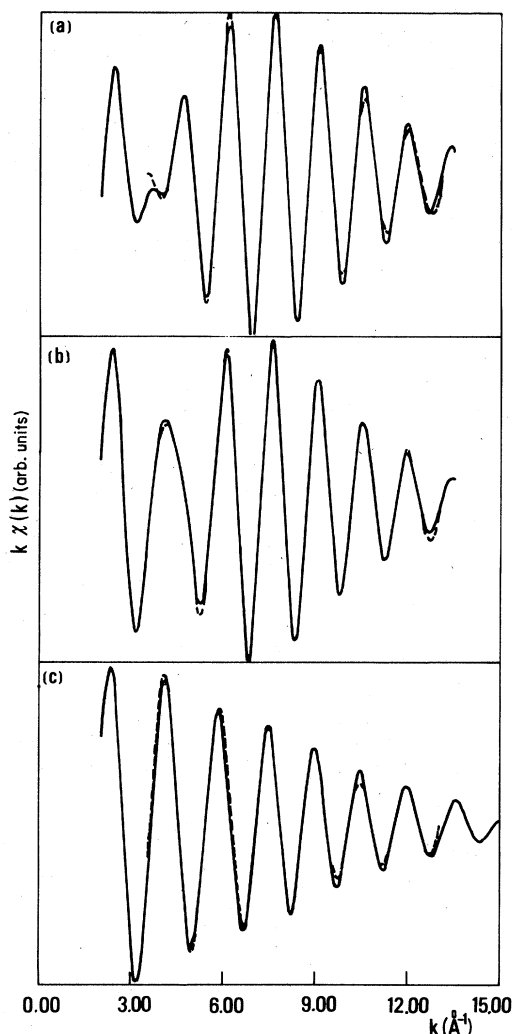


FIG. 9. Comparison of the experimental Fourier-filtered $k\chi(k)$ with the result of a fit obtained as discussed in the text.

TABLE I. Numerical values of the parameters obtained from the fitting procedure. Column 1, Ge relative content as obtained by chemical analysis. Column 2, Ge relative content as obtained by the fit of the EXAFS data as discussed in the text. Column 3, bond distance of the Ge-Ge pair. Column 4, difference of the disorder factor of the Ge-Ge pair with respect to the model. Column 5, bond distance of the Ge-Si pair. Column 6, difference of the disorder factor of the Ge-Si pair with respect to the model. For the greatest Ge concentration we do not report the values for the Ge-Si pair, since its contribution is within the uncertainty of the technique.

% Ge	% Ge by EXAFS	R in Å Ge-Ge	$\Delta\sigma^2$ in 10^{-3} Å ²	$R_{\text{Si-Ge}}$ in Å	$\Delta\sigma^2$ in 10^{-3} Å ²
28	26	2.45	-0.21	2.37	-0.03
32	30	2.45	0.42	2.37	-0.20
62	62	2.45	-0.05	2.37	0.17
64	65	2.45	-0.73	2.38	0.74
77	89	2.45	-0.11	2.38	2.7
89	100	2.45	-0.09		

(a) the bond lengths are constant over the whole concentration range;

(b) the relative concentrations of the Ge-Ge and Ge-Si pairs are in excellent agreement with the results of the chemical analysis (compare columns one and two);

(c) $\Delta\sigma^2$ values obtained are so small that the disorder factor can be considered constant over the whole range of concentration.

IV. DISCUSSION

Our results on distances are the first direct determination of first-nearest-neighbor bond length in Ge-Si:H amorphous alloys. The value found for a Ge-Ge pair is the same as in pure amorphous and crystalline Ge, while the value for a Ge-Si pair is very close to the sum of the two covalent radii (2.39–2.40 Å). Both bond distances are concentration independent. The last result seems to be in contrast with diffraction results on crystalline Ge-Si alloys, where a linear dependence of the lattice parameter versus concentration (Vegard's law) is found.²⁵ This is due to the fact that the lattice parameter in a multicomponent crystalline alloy is determined by a concentration weighted mean of the partial pair-distribution function of the components. In EXAFS too, if one limits oneself to the consideration of the first peak in the Fourier spectra, one gets again a "mean" linear behavior as shown in Fig. 3. Nonetheless, the EXAFS capability of determining the partial distribution function around a single atom allows the complete determination of the single-bond distances.²⁶

In crystalline alloys the single-bond distances too are slightly concentration dependent as shown in $\text{Ga}_x\text{In}_{1-x}\text{As}$,²⁷ and in $\text{Cd}_x\text{Mn}_{1-x}\text{Te}$.²⁸ On the contrary, indication that in amorphous alloys the bond distances are concentration independent was found in a diffraction study of $\text{Ge}_x\text{Sn}_{1-x}$ at $x=0.5$ and 0.75 .²⁹ Our study confirms this result in a different tetrahedral system, showing that this concentration-independent bond distance is probably a general feature of the disordered alloys: i.e., the lack of long-range-order constraints allows the relaxation

of the distances to their "molecular" values.

As mentioned previously, from the knowledge of the average composition of the Ge first-nearest-neighbor shell it is possible to derive information on the short-range order in the alloy. As a matter of fact, different degrees of compositional disorder can be superimposed on the topological disorder in the amorphous alloys.³⁰ The local composition can be either (a) chemically ordered (in this case for, e.g., $x=0.5$ we would have Ge atoms surrounded by Si atoms only and vice versa), or (b) randomly mixed (in this second case the probability of finding Ge or Si atoms as first neighbors would be proportional to the atomic concentration), or (c) composed of small clusters of only Ge or only Si atoms forming separated phases on a microscopic scale.

That the situation (b) is the most likely to occur in GeSi alloys was inferred from the comparison of Raman spectra with the calculated phonon density of states.³¹ To our knowledge only one direct structural study has been performed³² on a single concentration of unhydrogenated Ge-Si amorphous alloy, whose experimental results were interpreted in terms of a random mixing. We believe that the excellent agreement found in the present study between the relative number of Ge-Ge and Ge-Si pairs in the first-coordination shell and the overall chemical composition of the alloy demonstrates that the random composition model is the correct one for these materials. In fact one would get a relative weight of the Ge-Ge pair much lower than the chemical concentration in case (a) and much higher in case (c).

As discussed previously, the disorder factors of the alloys studied do not vary appreciably with concentration and remain equal to the value of the two models, namely $\sigma^2=(0.5\pm 0.025)\times 10^{-2}$ Å². This result is not surprising if one examines separately the two contributions to the disorder factor, namely the thermal and the structural components.

As for the thermal component, it has been shown³³ that only the "uncorrelated" motion of the atoms contribute to the EXAFS σ^2 . In the case of covalent semiconductors this uncorrelated motion is well represented by a simple Einstein model.³⁴ Therefore one gets

$$\frac{\Delta\sigma_{\text{Ge-Ge}}^2}{\Delta\sigma_{\text{Ge-Si}}^2} = \frac{\langle u^2 \rangle_{\text{Ge-Ge}}}{\langle u^2 \rangle_{\text{Ge-Si}}} = \frac{(\langle n \rangle + \frac{1}{2})_{\text{Ge-Ge}} \mu_{\text{Ge-Si}} \omega_{\text{Ge-Si}}}{(\langle n \rangle + \frac{1}{2})_{\text{Ge-Si}} \mu_{\text{Ge-Ge}} \omega_{\text{Ge-Ge}}} \sim 1,$$

where $\langle n \rangle$ is the Bose-Einstein occupation number, $\mu_{\text{Ge-Ge}}$ and $\mu_{\text{Ge-Si}}$ are the reduced masses of the Ge-Ge and Ge-Si pairs, and $\omega_{\text{Ge-Si}}$ and $\omega_{\text{Ge-Ge}}$ are the frequencies of the phonon modes localized on the Ge-Si and Ge-Ge pairs. These frequencies are concentration independent and equal to 400 and 290 cm^{-1} , respectively, as shown from Raman measurements.³⁵ This indicates that the thermal parts of the disorder factor are the same for the two pairs and do not vary with concentration. Therefore we conclude that the thermal contribution in all alloys is equal to that of *a*-Ge:H, i.e., $\sigma^2 = (0.33 \pm 0.01) \times 10^{-2} \text{ \AA}^2$.

As a consequence of the above result the structural contribution is the same for the Ge-Ge and Ge-Si pairs over the whole concentration range studied and equal to $(0.16 \pm 0.025) \times 10^{-2} \text{ \AA}^2$. The physical meaning of this is

that the rms fluctuations of the bond distances are the same for the two pairs and equal to $4 \times 10^{-2} \text{ \AA}$. The explanation of its constancy with concentration is to be found in the likeness of the interaction elastic potentials in these materials, a consequence of their very close electronic structure. This closeness is reflected in the nearly equal values of the Keating potentials³⁶ in pure Ge and Si. This means that the energy increase for a given bond stretching is nearly the same in the Ge-Ge and Si-Si pairs. It is reasonable then to assume that the Ge-Si pair also has the same interacting potential and consequently the same rms fluctuations of bond distances.

ACKNOWLEDGMENTS

The authors are grateful to Laboratori Nazionali di Frascati machine staff for their collaboration during the experiment. The skillful technical assistance of L. Moretto and R. Moretto is acknowledged. Thanks are due to P. Frigeri of the CISE Laboratoires for the chemical analysis of the samples.

*Present address: Istituto di Struttura della Materia del Consiglio Nazionale delle Ricerche, Via E. Fermi 38, 00044 Frascati (Roma), Italy.

¹D. Hauschildt, R. Fischer, and W. Fuhs, *Phys. Status Solidi B* **102**, 563 (1980); J. Blake, R. W. Collins, G. Moddel, and W. Paul, *Phys. Rev. B* **25**, 7678 (1982); L. Chahed, C. Senemaud, M. L. Theye, J. Bulot, M. Galin, M. Gauthier, B. Bourdon, and M. Toulemonde, *Solid State Commun.* **45**, 649 (1983).

²Y. Yukimoto, *Amorphous Semiconductor Technologies and Devices*, edited by Y. Hamakawa (North-Holland, New York, 1983), Vol. 6.

³For a general review on EXAFS see, e.g., P. A. Lee, P. H. Citrin, P. Eisenberger, and B. M. Kincaid, *Rev. Mod. Phys.* **53**, 769 (1981); T. M. Hayes and J. B. Boyce, in *Solid State Physics*, edited by H. Ehrenreich, F. Seitz, and D. Turnbull (Academic, New York, 1983), Vol. 37, p. 173.

⁴D. Della Sala, P. Fiorini, C. Giovannella, and F. Evangelisti, *Phys. Status Solidi B* **126**, 456 (1984).

⁵Laboratori Nazionali di Frascati Annual Report, 1979 and 1981.

⁶E. A. Stern and K. Kim, *Phys. Rev. B* **23**, 3781 (1981).

⁷F. Comin, L. Incoccia, and S. Mobilio, *J. Phys. E* **16**, 83 (1983).

⁸B. K. Teo and P. A. Lee, *J. Am. Chem. Soc.* **101**, 2815 (1979).

⁹D. E. Sayers, E. A. Stern, and F. W. Lytle, *Phys. Rev. Lett.* **27**, 1204 (1971).

¹⁰S. Mobilio and L. Incoccia, *Nuovo Cimento D* **3**, 846 (1984).

¹¹E. A. Stern, *Phys. Rev. B* **10**, 3027 (1974).

¹²E. A. Stern, B. A. Bunker, and S. M. Heald, *Phys. Rev. B* **21**, 5521 (1980).

¹³P. H. Citrin, P. Eisenberger, and B. M. Kincaid, *Phys. Rev. Lett.* **36**, 1346 (1976).

¹⁴P. Eisenberger and B. Lengeler, *Phys. Rev. B* **22**, 3551 (1980).

¹⁵D. E. Sayers, F. W. Lytle, and E. A. Stern, *J. Non-Cryst. Solids* **8**, 401 (1972).

¹⁶T. M. Hayes, *J. Non-Cryst. Solids* **31**, 57 (1978).

¹⁷P. Rabe, G. Tolkiehn, and A. Werner, *J. Phys. C* **12**, L545 (1979).

¹⁸F. Evangelisti, M. G. Proietti, A. Balzarotti, F. Comin, L. Incoccia, and S. Mobilio, *Solid State Commun.* **37**, 413 (1981).

¹⁹E. D. Crozier and A. J. Seary, *Can. J. Phys.* **59**, 876 (1981).

²⁰E. A. Stern, C. E. Bouldin, B. Von Roedern, and J. Azoulai, *Phys. Rev. B* **27**, 6557 (1983).

²¹M. A. Paesler, D. E. Sayers, R. Tsu, and J. Gonzalez-Hernandez, *Phys. Rev. B* **28**, 4550 (1983).

²²G. Martens, P. Rabe, N. Schwentner, and A. Werner, *Phys. Rev. B* **17**, 1481 (1978).

²³L. Incoccia and S. Mobilio, *Nuovo Cimento D* **3**, 867 (1984).

²⁴J. C. Rehr, H. Meuth, S. Sevillano, and S. H. Chow (unpublished).

²⁵R. Johnson and S. M. Christian, *Phys. Rev.* **95**, 560 (1954).

²⁶J. C. Mikkelsen Jr. and J. B. Boyce, *Phys. Rev. B* **28**, 7130 (1983).

²⁷J. C. Mikkelsen Jr. and J. B. Boyce, *Phys. Rev. Lett.* **49**, 1412 (1982).

²⁸A. Balzarotti, M. Czyzyk, A. Kisiel, N. Motta, M. Podgorny, and Zimnal-Starnawska, *Phys. Rev. B* **30**, 2295 (1984).

²⁹R. J. Temkin, G. A. N. Connell, and W. Paul, *Solid State Commun.* **11**, 1591 (1978).

³⁰G. A. N. Connell, and G. Lucovsky, *J. Non-Cryst. Solids* **31**, 123 (1978).

³¹B. K. Agrawal, *Solid State Commun.* **37**, 271 (1981).

³²N. J. Shevchik, J. S. Lannin, and J. Tejada, *Phys. Rev. B* **7**, 3987 (1973).

³³G. Beni and P. M. Platzman, *Phys. Rev. B* **14**, 1514 (1976).

³⁴J. J. Rehr (unpublished).

³⁵S. Minomura, K. Tsugi, M. Wakagi, T. Ishidate, K. Inoue, and M. Shibuya, *J. Non-Cryst. Solids* **59-60**, 541 (1983).

³⁶P. N. Keating, *Phys. Rev.* **145**, 637 (1966).